ISSN: 2152-1972

The IRM Quarterly
Fall 2016, Vol. 26 No.3

The do's and don'ts of inclination shallowing corrections

Dario Bilardello
Institute for Rock Magnetism
dario@umn.edu

Essential Introduction

Increasing recognition of inclination shallowing in sedimentary paleomagnetic records, together with developments of inclination correction techniques over the past few years have generated widespread interest in the topic. Inclination corrections are now being quasi-routinely applied thanks to the ease of particular techniques, and so the time is right for a brief review of inclination error and its relative correction.

Trustworthy evidence of depositional inclination shallowing was first obtained in the laboratory, and certain key studies provided the first attempts at quantifying the inclination error and investigating its causes. King (1955) formulated the most widely used expression for inclination shallowing, relating the remanent inclination (I_R) to the ambient field inclination (I_F) with the tangent-tangent equation:

$$\tan(I_R) = f \tan(I_F)$$

where f is the flattening (or shallowing) factor, and was determined to be ~0.4 in the experiments he conducted. King (1955) postulated that shallowing arose from a flattening of the more anisotropic particles within the bedding plane, whereas the spherical particles more "accurately" record the field inclination, and thus introduced the "plates and spheres" model in the literature. Note however, that "plate-" and "sphere-" like behavior was also believed to be dependent on the intrinsic magnetization of the particles, in such a way that imperfectly spherical particles with weak magnetizations would still align with their long axes (and moments) horizontal, even in strong fields (King, 1955).

Shortly later, Griffiths et al. (1960) introduced the possibility that rolling of the spherical particles, due to asperities in the sediment surface, could lead to shallower than expected inclinations. In their model, the flattening factor represents the average angle φ through which the grains roll, and is given by

$$f = \cos(\varphi)/(1+\cos(\varphi)).$$

Tauxe and Kent (1984) studied the remanent intensity and inclination of disaggregated natural sediment containing a mixture of hematite and magnetite redeposited in the laboratory and determined their f factor as 0.55. They also postulated that the f factor can be predicted by the ratio R of the remanent intensity acquired in vertical fields (contribution of the spheres) to the remanent intensity acquired in horizontal fields (contribution of both plates and spheres). Tauxe and Kent (1984) also popularized the tangent-tangent relationship of King (1955) by generating the known I_0 (or I_R) versus I_F plot (figure 1). The plot highlights the observation of inclination shallowing being more pronounced for intermediate field inclinations.

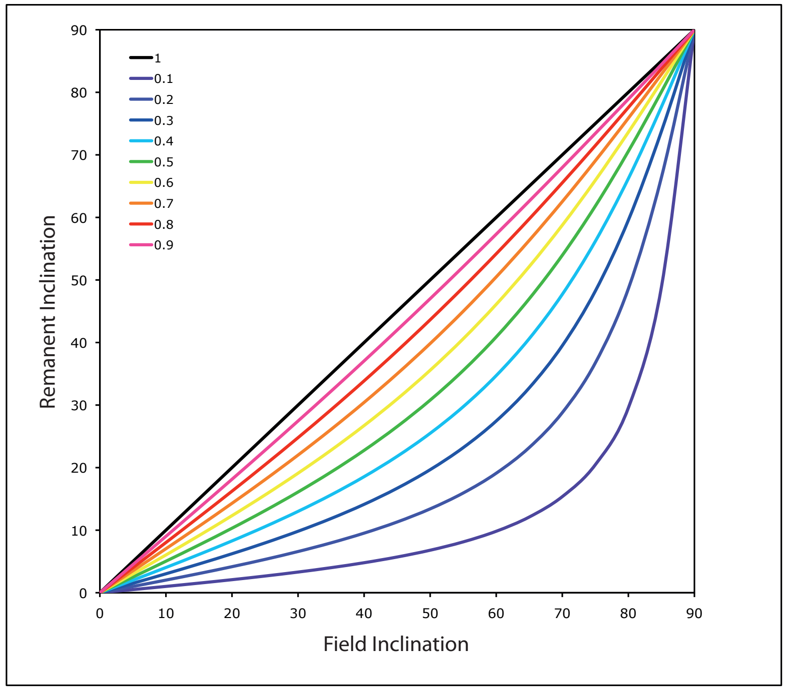

Fig. 1. Relation of the remanent inclination to the field inclination for flattening factors ranging between 1 (no inclination shallowing) and 0.1. The relationship highlights how inclination shallowing is maximized at mid-latitudes (intermediate field inclinations).

The consequences of inclination shallowing for paleomagnetic studies lie in the positioning of paleopoles and consequently in the reconstructed continent positions. The inclination error increases the co-latitude and makes paleopoles appear far-sighted, effectively biasing paleogeographies towards low latitudes, hence the need to correct for the error.

Anisotropy-based inclination corrections

Jackson et al. (1991) were the first to propose an inclination correction technique based on the bulk anisot-

cont'd. on pg. 8..

Visiting Fellow Report

Application of magnetic techniques to lateral hydrocarbon migration - Lower Tertiary reservoir systems, UK North Sea

S. Adesope Badejo
Imperial College London
Departement of Earth Science and Engineering
sopebadejo@gmail.com

High-wavenumber magnetic anomalies discovered over oil fields have been interpreted as showing the presence of near surface magnetic minerals (Donovan et al., 1984; Foote, 1984; Saunders and Terry, 1985). Pyrolysis experiments recreated the catagenesis environment of oil source rocks, the results showed peak magnetic mineral formation at 250°C (Abubakar et al., 2015). The magnetic minerals formed were < 10 nm which are small enough to get through the pore throat of the reservoir. Our study aims to use the magnetic mineral distribution to investigate hydrocarbon migration pathways. The Lower Tertiary reservoir system in the Central Graben of the UK North Sea is the study area. This area has been selected because the Tertiary sandstones are not deformed, they are laterally continuous which facilities long distance lateral migration of up to 50 km for oil and 32 km for gas (Cayley, 1987; Kubala et al., 2003). Samples were obtained from the British Geological Survey (BGS) in Keyworth, UK. Samples are selected based on susceptibility readings and geological observations (water wet sandstone, oil stained sandstones, siltstone and shale)

Isothermal remanent magnetization curves (IRM), backfield curves, hysteresis loops and first-order reversal curves (FORCs) were measured at room temperature (RT) using a Princeton Measurements Vibrating Sample Magnetometer (VSM) at Imperial College London for magnetic mineral characterization. The results showed varying grain sizes from superparamagnetic grains (SP) to pseudo- single domain grains (PSD) and a mixture of minerals with low- coercivity phase (possibly magnetite or pyrrhotite) and high-coercivity phase (possibly hematite or goethite). The visit to the IRM was designed to determine the morphology, abundance, mineralogy and size of the magnetic minerals present in the reservoir rocks.

During the visit to IRM, low temperature (300K- 10K) and high temperature experiments (30°C-700°C) were carried out using Magnetic Properties Measurement System (MPMS) and high temperature Kappabridge respectively. For the low temperature experiments, low temperature demagnetisation was performed after imparting a saturation isothermal remanent magnetization at room temperature (RTSIRM LTD) for most of the samples while for a few samples this was done along with field cooling (FC), zero field cooling (ZFC) remanence measurements. For the high temperature experiments, susceptibility was measured as the sample was heated from RT to a temperature (< 700°C) and as it cools to RT. This heating and cooling was done in 5 steps (250°C, 350°C, 450°C, 550°C and 700°C). This was done to identify the presence of iron sulphides as they tend to alter to magnetite at temperatures above 300°C.

The Verwey transition (Dunlop and Özdemir, 1997) is visible on the RTSIRM LTD curves for most samples but is suppressed in the FC-ZFC curves (Figure 1a). The FC-ZFC curves were vital in the identification of siderite as it displays a steep decay in remanence at its Néel temperature (37K) with the FC remanence being at least two times higher than the ZFC remanence (Frederichs et al., 2003). In some samples the RTSIRM LTD curves showed an increase in remanence on cooling from RT (Figure 1b) which suggests the presence of goethite (Dekkers, 1989). This increase of remanence suppresses the Verwey transition and any possible pyrrhotite transition between 30- 34K (Rochette et al., 1990). It has been difficult to identify pyrrhotite as the presence of other minerals (including siderite) suppress its transition

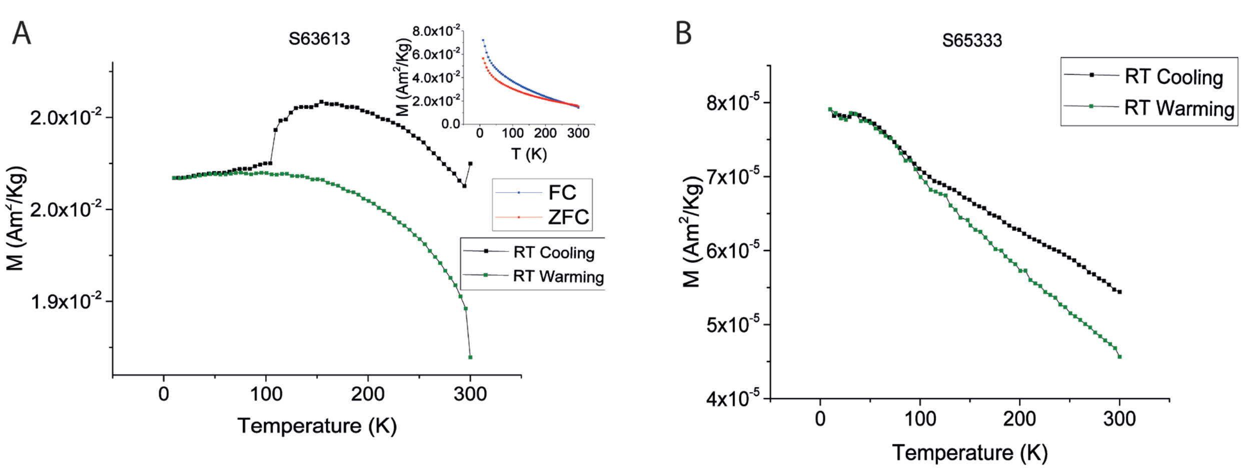

Fig. 1: Figure 1 a. measurement of remanence after FC (blue) and ZFC (red) along with RTSIRM LTD cooling (black) and warming (green) curves. b RTSIRM LTD cooling (black) and warming (green) curves.

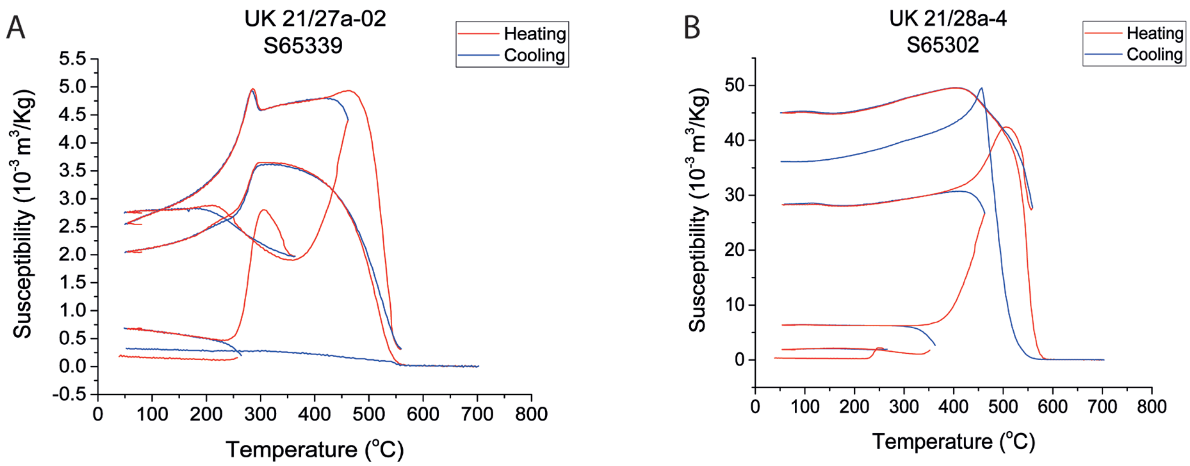

Fig. 2: Susceptibility as a function of temperature: heating curve (red) along with cooling curve (blue).

and in one case the drop in remanence is defined by one or two measurement points only, which could be noise. Hematite was identified in a few samples by its Morin transition (Dunlop and Özdemir., 1997). Magnetite was the most abundant mineral while hematite was the least abundant.

Two patterns were observed with the high temperature experiments. The first pattern (Figure 2a) shows an increase in susceptibility at temperatures above 250°C then a steep drop in susceptibility between 300- 350°C which coincides with the Curie temperature of greigite and Curie & Néel temperature of pyrrhotite (Dunlop and Özdemir, 1997). The steep drop is then followed by an increase in susceptibility suggesting the iron sulphides alter to magnetite which is proven by a second steep drop in susceptibility around 580°C. The first pattern suggests the samples have a mixture of iron sulphides with more ferrimagnetic iron sulphides than paramagnetic iron sulphides (pyrite). The second pattern (Figure 2b) shows and increase in susceptibility around 300°C then a steep drop in susceptibility between 560-590°C, suggesting the iron sulphides alters to magnetite. This suggest the samples have a mixture of iron sulphides with more paramagnetic iron sulphides than ferrimagnetic iron sulphides.

The results from IRM confirms magnetite, pyrrhotite, pyrite and siderite are precipitated in hydrocarbon reducing conditions. Low temperature data highlighted the presence of maghemite in some samples, we believe the magnetite precipitated oxidises to maghemite as the samples are exposed to air in the core store. Goethite may be one of the minerals precipitated but a goethite test is needed to verify its presence. Our results hint at an increasing presence of ferrimagnetic iron sulphides along the known hydrocarbon migration pathway. More work is needed to verify this.

I would like to thank Dario Bilardello, Mike Jackson and Peter Solheid for their assistance and helpful suggestions during my visit.

List of References

Abubakar, R., Muxworthy, A. R., Sephton, M. A., Southern, P., Watson, J. S., Fraser, A. J., and Almeida, T. P., 2015, Formation of magnetic minerals in hydrocarbon-generation conditions: Marine and Petroleum Geology, v. 68, Part A, p. 509-519.

Cayley, G., 1987, Hydrocarbon migration in the central North Sea: Petroleum geology of north west Europe, p. 549-555.

Dekkers, M. J., 1989, Magnetic Properties of Natural Goethite—II. TRM Behaviour During Thermal and Alternating Field Demagnetization and Low-Temperature Treatment: Geophysical Journal International, v. 97, no. 2, p. 341-355.

Donovan, T. J., Hendricks, J. D., Roberts, A. A., and Eliason, P. T., 1984, Low-altitude aeromagnetic reconnaissance for petroleum in the Arctic National Wildlife Refuge, Alaska: Geophysics, v. 49, no. 8, p. 1338-1353.

Dunlop, D. J., and Özdemir., Ö., 1997, Rock Magnetism, Cambridge University Press.

Foote, R. S., 1984, Significance of near-surface magnetic anomalies: Unconventional Methods in Exploration for Petroleum and Natural Gas. Institute for Study of Earth and Man, Southern Methodist University, Dallas, p. 12-24.

Frederichs, T., von Dobeneck, T., Bleil, U., and Dekkers, M. J., 2003, Towards the identification of siderite, rhodochrosite, and vivianite in sediments by their low-temperature magnetic properties: Physics and Chemistry of the Earth, Parts A/B/C, v. 28, no. 16–19, p. 669-679.

Kubala, M., Bastow, M., Thompson, S., Scotchman, I., and Oygard, K., 2003, Geothermal regime, petroleum generation and migration in The Millennium Atlas: Petroleum Geology of the Central and Northern North Sea. Geological Society, London: Evans, D, Graham, C, Armour, A, and Bathurst, P (editors and co-ordinators).(London: The Geological Society of London), p. 289-215.

Rochette, P., Fillion, G., Mattéi, J.-L., and Dekkers, M. J., 1990, Magnetic transition at 30–34 Kelvin in pyrrhotite: insight into a widespread occurrence of this mineral in rocks: Earth and Planetary Science Letters, v. 98, no. 3, p. 319-328.

Saunders, D., and Terry, S., 1985, Onshore exploration using the new geochemistry and geomorphology: Oil & Gas Journal, v. 83, no. 37, p. 126-130.

Current Articles

A list of current research articles dealing with various topics in the physics and chemistry of magnetism is a regular feature of the IRM Quarterly. Articles published in familiar geology and geophysics journals are included; special emphasis is given to current articles from physics, chemistry, and materials-science journals. Most are taken from ISI Web of Knowledge, after which they are subjected to Procrustean culling for this newsletter. An extensive reference list of articles (primarily about rock magnetism, the physics and chemistry of magnetism, and some paleomagnetism) is continually updated at the IRM. This list, with more than 10,000 references, is available free of charge. Your contributions both to the list and to the Current Articles section of the IRM Quarterly are always welcome.

Archeomagnteism

Carrancho, A., A. H. Lagunilla, and J. M. Verges (2016), Three archaeomagnetic applications of archaeological interest to the study of burnt anthropogenic cave sediments, Quaternary International, 414, 244-257.

Terra-Nova, F., H. Amit, G. A. Hartmann, and R. I. F. Trindade (2016), Using archaeomagnetic field models to constrain the physics of the core: robustness and preferred locations of reversed flux patches, Geophysical Journal International, 206(3), 1890-1913.

Zykin, V. S., V. S. Zykina, and L. G. Smolyaninova (2016), Debatable Aspects of Initial Human Colonization of Siberia and Age of the Karama Site in the Altai Mountains, Stratigraphy and Geological Correlation, 24(3), 313-330.

Biomagnetism

Abrajevitch, A., L. M. Kondratyeva, E. M. Golubeva, K. Kodama, and R. S. Hori (2016), Magnetic properties of iron minerals produced by natural iron- and manganese-reducing groundwater bacteria, Geophysical Journal International, 206(2), 1340-1351.

Environmental magnetism and Climate

Dare, M. S., J. A. Tarduno, R. K. Bono, R. D. Cottrell, J. S. Beard, and K. P. Kodama (2016), Detrital magnetite and chromite in Jack Hills quartzite cobbles: Further evidence for the preservation of primary magnetizations and new insights into sediment provenance, Earth and Planetary Science Letters, 451, 298-314.

Fayol, N., M. Jebrak, and L. B. Harris (2016), The magnetic signature of Neoarchean alkaline intrusions and their related gold deposits: Significance and exploration implications, Precambrian Research, 283, 13-23.

Gutierrez, L., V. Barron, M. Andres-Verges, C. J. Serna, S. Veintemillas-Verdaguer, M. P. Morales, and F. J. Lazaro (2016), Detailed magnetic monitoring of the enhanced magnetism of ferrihydrite along its progressive transformation into hematite, Journal of Geophysical Research-Solid Earth, 121(6), 4118-4129.

Han, F., F. X. Wang, J. H. Li, H. F. Qin, C. L. Deng, and Y. X. Pan (2016), Identification of magnetic minerals in surface sediments of Miyun Lake, Beijing, Chinese Journal of Geophysics-Chinese Edition, 59(8), 2937-2948.

Hernandez-Bernal, M. D., J. Morales, P. Corona-Chavez, A. Goguitchaichvili, and F. Bautista (2016), Combined rock-magnetic and geochemical characterization of Angangueo mining district, central Mexico, Environmental Earth Sciences, 75(18).

Jung, H. B., H. F. Xu, H. Konishi, and E. E. Roden (2016), Role of nano-goethite in controlling U(VI) sorption-desorption in subsurface soil, Journal of Geochemical Exploration, 169, 80-88.

Kasper-Zubillaga, J. J., C. L. Lopez, and C. Munoz (2016), Provenance of opaque minerals in coastal sands, western Gulf of Mexico, Mexico, Boletin De La Sociedad Geologica Mexicana, 68(2), 323-338.

Kawamura, N., Y. Amano, and N. Ishikawa (2016), Seasonal changes in magnetic parameters of sediments with changing redox conditions in Hiroshima Bay, Japan, Geochemistry Geophysics Geosystems, 17(7), 2687-2699.

Kikuchi, S., H. Makita, U. Konno, F. Shiraishi, A. Ijiri, K. Takai, M. Maeda, and Y. Takahashi (2016), Limited reduction of ferrihydrite encrusted by goethite in freshwater sediment, Geobiology, 14(4), 374-389.

Li, B., Y. Wang, H. X. Zhong, J. Y. Zhang, S. Li, X. J. Li, and H. F. Gao (2016), Magnetic properties of turbidites in the Huatung Basin and their environmental implications, Chinese Journal of Geophysics-Chinese Edition, 59(9), 3330-3342.

Liu, Z. F., G. J. Wei, X. S. Wang, C. S. Jin, and Q. S. Liu (2016), Quantifying paleoprecipitation of the Luochuan and Sanmenxia Loess on the Chinese Loess Plateau, Palaeogeography Palaeoclimatology Palaeoecology, 459, 121-130.

Lozinski, M., P. Ziolkowski, and A. Wysocka (2016), Lithofacies and terrestrial sedimentary environments in AMS measurements: a case study from the Neogene of the Oravica River section, Cimhova, Slovakia, Geological Quarterly, 60(2), 259-272.

Mahmud, S. A., S. Naseem, M. Hall, and K. A. Almalki (2016), Geochemistry of Late Cambrian-Early Ordovician fluvial to shallow marine sandstones, western Tasmania, Australia: Implications for provenance, weathering, tectonic settings, and chemostratigraphy, Geochemical Journal, 50(2), 197-210.

Manga, V. E., C. M. Agyingi, and C. E. Suh (2016), Trace element behaviour in soils developed along the slopes of Mt. Cameroon, West Africa, Geochemical Journal, 50(3), 267-280.

Maxbauer, D. P., J. M. Feinberg, D. L. Fox, and W. C. Clyde (2016), Magnetic minerals as recorders of weathering, diagenesis, and paleoclimate: A core-outcrop comparison of Paleocene-Eocene paleosols in the Bighorn Basin, WY, USA, Earth and Planetary Science Letters, 452, 15-26.

Minyuk, P. S., and V. Y. Borkhodoev (2016), Geochemistry of sediments from Lake Grand, Northeast Russia, Geochemistry International, 54(9), 807-816.

Mohanty, S. P., and S. Nanda (2016), Geochemistry of a paleosol horizon at the base of the Sausar Group, central India: Implications on atmospheric conditions at the Archean-Paleoproterozoic boundary, Geoscience Frontiers, 7(5), 759-773.

Och, L. M., B. Muller, C. Marz, A. Wichser, E. G. Vologina, and M. Sturm (2016), Elevated uranium concentrations in Lake Baikal sediments: Burial and early diagenesis, Chemical Geology, 441, 92-105.

Pan, B. T., H. L. Pang, H. S. Gao, E. Garzanti, Y. Zou, X. P. Liu, F. Q. Li, and Y. X. Jia (2016), Heavy-mineral analysis and provenance of Yellow River sediments around the China Loess Plateau, Journal of Asian Earth Sciences, 127, 1-11.

Profe, J., B. Zolitschka, W. Schirmer, M. Frechen, and C. Ohlendorf (2016), Geochemistry unravels MIS 3/2 paleoenvironmental dynamics at the loess-paleosol sequence Schwalbenberg II, Germany, Palaeogeography Palaeoclimatology Palaeoecology, 459, 537-551.

Raiswell, R., et al. (2016), Potentially bioavailable iron delivery by iceberg-hosted sediments and atmospheric dust to

the polar oceans, Biogeosciences, 13(13), 3887-3900.
Rogozin, D. Y., D. A. Balaev, S. V. Semenov, K. A. Shaikhutdinov, and O. A. Bayukov (2016), Magnetic properties of bottom sediments from Meromectic Shira Lake (Siberia, Russia), Doklady Earth Sciences, 469(2), 819-823.
Wang, H. Y., Y. Q. Song, Y. Cheng, Y. Luo, C. N. Zhang, Y. S. Gao, A. A. Qiu, L. Deng, and H. Y. Liu (2016), Mineral magnetism and other characteristics of sediments from a sub-alpine lake (3080 m a.s.l.) in central east China and their implications on environmental changes for the last 5770 years, Earth and Planetary Science Letters, 452, 44-59.
Wu, X. D., Y. Wang, L. Bian, and J. Shen (2016), Diagenetic effects on magnetic minerals in a Holocene lacustrine sediment core from Huguangyan maar lake, southeast China, Geophysical Journal International, 206(3), 1586-1598.
Xiang, F., Y. W. Wang, Y. Zhang, S. X. Li, J. Y. Wang, and Q. Fen (2016), Provenance of Detrital Magnetites from Quaternary Sediments in the Yichang Area and its Significance to the Birth of the Three Gorges, Yangtze River, Acta Geologica Sinica-English Edition, 90(3), 1063-1064.
Yue, W., J. T. Liu, D. Zhang, Z. H. Wang, B. C. Zhao, Z. Y. Chen, and J. Chen (2016), Magnetite with anomalously high Cr2O3 as a fingerprint to trace upper Yangtze sediments to the sea, Geomorphology, 268, 14-20.
Zan, J. B., X. M. Fang, W. L. Zhang, M. D. Yan, and T. Zhang (2016), Palaeoenvironmental and chronological constraints on the Early Pleistocene mammal fauna from loess deposits in the Linxia Basin, NE Tibetan Plateau, Quaternary Science Reviews, 148, 234-242.

Fundamental Rock and Mineral Magnetism

Halama, M., E. D. Swanner, K. O. Konhauser, and A. Kappler (2016), Evaluation of siderite and magnetite formation in BIFs by pressure-temperature experiments of Fe(III) minerals and microbial biomass, Earth and Planetary Science Letters, 450, 243-253.
Hu, P. X., Z. X. Jiang, Q. S. Liu, D. Heslop, A. P. Roberts, J. Torrent, and V. Barron (2016), Estimating the concentration of aluminum-substituted hematite and goethite using diffuse reflectance spectrometry and rock magnetism: Feasibility and limitations, Journal of Geophysical Research-Solid Earth, 121(6), 4180-4194.
Jiang, Z. X., Q. S. Liu, X. Zhao, A. P. Roberts, D. Heslop, V. Barron, and J. Torrent (2016), Magnetism of Al-substituted magnetite reduced from Al-hematite, Journal of Geophysical Research-Solid Earth, 121(6), 4195-4210.
Maxbauer, D. P., J. M. Feinberg, and D. L. Fox (2016), MAX UnMix: A web application for unmixing magnetic coercivity distributions, Computers & Geosciences, 95, 140-145.
Plado, J., L. Ainsaar, M. Dmitrijeva, K. Poldsaar, S. Ots, L. J. Pesonen, and U. Preeden (2016), Magnetic susceptibility of Middle Ordovician sedimentary rocks, Pakri Peninsula, NW Estonia, Estonian Journal of Earth Sciences, 65(3), 125-137.
Rashidov, V. A., O. V. Pilipenko, and V. V. Petrova (2016), Rock Magnetic and Petrographical-Mineralogical Studies of the Dredged Rocks from the Submarine Volcanoes of the Sea-of-Okhotsk Slope within the Northern Part of the Kuril Island Arc, Izvestiya-Physics of the Solid Earth, 52(4), 550-571.
Reis, A. L. A., V. C. Oliveira, E. Yokoyama, A. C. Bruno, and J. M. B. Pereira (2016), Estimating the magnetization distribution within rectangular rock samples, Geochemistry Geophysics Geosystems, 17(8), 3350-3374.
Sato, M., Y. Yamamoto, T. Nishioka, K. Kodama, N. Mochizuki, and H. Tsunakawa (2016), Hydrostatic pressure effect on magnetic hysteresis parameters of pseudo-single-domain magnetite, Geochemistry Geophysics Geosystems, 17(7), 2825-2834.

High Pressure Magnetism

Bezaeva, N. S., D. A. Chareev, P. Rochette, M. Kars, J. Gattacceca, J. M. Feinberg, R. A. Sadykov, D. M. Kuzina, and S. N. Axenov (2016), Magnetic characterization of non-ideal single-domain monoclinic pyrrhotite and its demagnetization under hydrostatic pressure up to 2 GPa with implications for impact demagnetization, Physics of the Earth and Planetary Interiors, 257, 79-90.
Reznik, B., A. Kontny, J. Fritz, and U. Gerhards (2016), Shock-induced deformation phenomena in magnetite and their consequences on magnetic properties, Geochemistry Geophysics Geosystems, 17(6), 2374-2393.

Magnetic Fabrics and Anisotropy

Airoldi, G. M., J. D. Muirhead, S. M. Long, E. Zanella, and J. D. L. White (2016), Flow dynamics in mid-Jurassic dikes and sills of the Ferrar large igneous province and implications for long-distance magma transport, Tectonophysics, 683, 182-199.
Ferre, E. C., Y. M. Chou, R. L. Kuo, E. C. Yeh, N. R. Leibovitz, A. L. Meado, L. Campbell, and J. W. Geissman (2016), Deciphering viscous flow of frictional melts with the mini-AMS method, Journal of Structural Geology, 90, 15-26.
Ferreira, F., L. Lagoeiro, L. F. G. Morales, C. G. de Oliveira, P. Barbosa, C. Avila, and G. C. G. Cavalcante (2016), Texture development during progressive deformation of hematite aggregates: Constraints from VPSC models and naturally deformed iron oxides from Minas Gerais, Brazil, Journal of Structural Geology, 90, 111-127.
Issachar, R., T. Levi, V. Lyakhovsky, S. Marco, and R. Weinberger (2016), Improving the method of low-temperature anisotropy of magnetic susceptibility (LT-AMS) measurements in air, Geochemistry Geophysics Geosystems, 17(7), 2940-2950.
Salazar, C. A., C. Bustamante, and C. J. Archanjo (2016), Magnetic fabric (AMS, AAR) of the Santa Marta batholith (northern Colombia) and the shear deformation along the Caribbean Plate margin, Journal of South American Earth Sciences, 70, 55-68.

Paleointensity and records of the geomagnetic field

Constable, C., M. Korte, and S. Panovska (2016), Persistent high paleosecular variation activity in southern hemisphere for at least 10 000 years, Earth and Planetary Science Letters, 453, 78-86.
Goguitchaichvili, A., A. Caccavari, M. Calvo-Rathert, J. Morales, M. C. Solano, G. Vashakidze, H. Y. He, and N. Vegas (2016), Absolute paleointensity determinations by using of conventional double-heating and multispecimen approaches on a Pliocene lava flow sequence from the Lesser Caucasus, Physics of the Earth and Planetary Interiors, 257, 158-170.
Herrero-Bervera, E., D. Krasa, and M. J. Van Kranendonk (2016), A whole rock absolute paleointensity determination of dacites from the Duffer Formation (ca. 3.467 Ga) of the Pilbara Craton, Australia: An impossible task?, Physics of the Earth and Planetary Interiors, 258, 51-62.
Lhuillier, F., S. A. Gilder, M. Wack, K. He, N. Petersen, B. S. Singer, B. R. Jicha, A. J. Schaen, and D. Colon (2016), More stable yet bimodal geodynamo during the Cretaceous superchron?, Geophysical Research Letters, 43(12), 6170-6177.
Meert, J. G., N. M. Levashova, M. L. Bazhenov, and E. Landing (2016), Rapid changes of magnetic Field polarity in the late Ediacaran: Linking the Cambrian evolutionary radiation and increased UV-B radiation, Gondwana Research,

34, 149-157.
Xu, M., and M. A. Tivey (2016), Investigation of a marine magnetic polarity reversal boundary in cross section at the northern boundary of the Kane Megamullion, Mid-Atlantic Ridge, 23 degrees 40 ' N, Journal of Geophysical Research-Solid Earth, 121(5), 3161-3176.

Paleomagnetism

Barnett-Moore, N., M. Hosseinpour, and S. Maus (2016), Assessing discrepancies between previous plate kinematic models of Mesozoic Iberia and their constraints, Tectonics, 35(8), 1843-1862.
Crespo-Blanc, M., M. Comas, and J. C. Balanya (2016), Clues for a Tortonian reconstruction of the Gibraltar Arc: Structural pattern, deformation diachronism and block rotations, Tectonophysics, 683, 308-324.
Domeier, M. (2016), A plate tectonic scenario for the Iapetus and Rheic oceans, Gondwana Research, 36, 275-295.
Eagles, G. (2016), Plate kinematics of the Rocas Verdes Basin and Patagonian orocline, Gondwana Research, 37, 98-109.
Evans, D. A. D., R. V. Veselovsky, P. Y. Petrov, A. V. Shatsillo, and V. E. Pavlov (2016), Paleomagnetism of Mesoproterozoic margins of the Anabar Shield: A hypothesized billion-year partnership of Siberia and northern Laurentia, Precambrian Research, 281, 639-655.
Fairchild, L. M., N. L. Swanson-Hysell, and S. M. Tikoo (2016), A matter of minutes: Breccia dike paleomagnetism provides evidence for rapid crater modification, Geology, 44(9), 723-726.
Fazzito, S. Y., and A. E. Rapalini (2016), Magnetic properties of the remagnetized Middle-Ordovician limestones of the Ponon Trehue Formation (San Rafael Block, central-western Argentina): Insights into the Permian widespread Sanrafaelic overprint, Journal of South American Earth Sciences, 70, 279-297.
Franceschinis, P. R., A. E. Rapalini, M. P. Escayola, and T. Luppo (2016), Paleomagnetic studies on the late Ediacaran - Early Cambrian Puncoviscana and the late Cambrian Campanario formations, NW Argentina: New paleogeographic constraints for the Pampia terrane, Journal of South American Earth Sciences, 70, 145-161.
Heslop, D., and A. P. Roberts (2016), Estimation and propagation of uncertainties associated with paleomagnetic directions, Journal of Geophysical Research-Solid Earth, 121(4), 2274-2289.
Hu, X. M., E. Garzanti, J. G. Wang, W. T. Huang, W. An, and A. Webb (2016), The timing of India-Asia collision onset - Facts, theories, controversies, Earth-Science Reviews, 160, 264-299.
Ivanov, S. A., and S. A. Merkuryev (2016), The Possibilities of Paleomagnetic and Geohistorical Analyses of "Tiny Wiggles" Short-Period Marine Magnetic Anomalies, Geomagnetism and Aeronomy, 56(3), 367-379.
Japas, M. S., G. H. Re, S. Oriolo, and J. F. Vilas (2016), Basement-involved deformation overprinting thin-skinned deformation in the Pampean flat-slab segment of the southern Central Andes, Argentina, Geological Magazine, 153(5-6), 1042-1065.
Kilian, T. M., K. R. Chamberlain, D. A. D. Evans, W. Bleeker, and B. L. Cousens (2016), Wyoming on the run-Toward final Paleoproterozoic assembly of Laurentia, Geology, 44(10), 863-866.
Kirscher, U., J. Prieto, V. Bachtadse, H. A. Aziz, G. Doppler, M. Hagmaier, and M. Bohme (2016), A biochronologic tie-point for the base of the Tortonian stage in European terrestrial settings: Magnetostratigraphy of the topmost Upper Freshwater Molasse sediments of the North Alpine Foreland Basin in Bavaria (Germany), Newsletters on Stratigraphy, 49(3), 445-467.
Koymans, M. R., C. G. Langereis, D. Pastor-Galan, and D. J. J. van Hinsbergen (2016), Paleomagnetism.org: An online multi-platform open source environment for paleomagnetic data analysis, Computers & Geosciences, 93, 127-137.
Lang, K. A., K. W. Huntington, R. Burmester, and B. Housen (2016), Rapid exhumation of the eastern Himalayan syntaxis since the late Miocene, Geological Society of America Bulletin, 128(9-10), 1403-1422.
Li, Z. Y., L. Ding, P. C. Lippert, P. P. Song, Y. H. Yue, and D. J. J. van Hinsbergen (2016), Paleomagnetic constraints on the Mesozoic drift of the Lhasa terrane (Tibet) from Gondwana to Eurasia, Geology, 44(9), 727-730.
Lu, H. J., B. H. Fu, P. L. Shi, Y. X. Ma, and H. B. Li (2016), Constraints on the uplift mechanism of northern Tibet, Earth and Planetary Science Letters, 453, 108-118.
Metelkin, D. V., V. A. Vernikovsky, T. Y. Tolmacheva, N. Y. Matushkin, A. I. Zhdanova, and S. A. Pisarevsky (2016), First paleomagnetic data for the New Siberian Islands: Implications for Arctic paleogeography, Gondwana Research, 37, 308-323.
Ran, B., X. X. Zhao, Z. F. Liu, C. S. Wang, L. D. Zhu, W. Jin, and Y. L. Li (2016), Cenozoic Vertical-Axis Rotations of the Hoh Xil Basin, Central-Northern Tibet, Acta Geologica Sinica-English Edition, 90(3), 858-869.
Ren, Q., S. H. Zhang, H. C. Wu, Z. K. Liang, X. J. Miao, H. Q. Zhao, H. Y. Li, T. S. Yang, J. L. Pei, and G. A. Davis (2016), Further paleomagnetic results from the similar to 155 Ma Tiaojishan Formation, Yanshan Belt, North China, and their implications for the tectonic evolution of the Mongol-Okhotsk suture, Gondwana Research, 35, 180-191.
Tanty, C., J. P. Valet, J. Carlut, F. Bassinot, and S. Zaragosi (2016), Acquisition of detrital magnetization in four turbidites, Geochemistry Geophysics Geosystems, 17(8), 3207-3223.
Tauxe, L., R. Shaar, L. Jonestrask, N. L. Swanson-Hysell, R. Minnett, A. A. P. Koppers, C. G. Constable, N. Jarboe, K. Gaastra, and L. Fairchild (2016), PmagPy: Software package for paleomagnetic data analysis and a bridge to the Magnetics Information Consortium (MagIC) Database, Geochemistry Geophysics Geosystems, 17(6), 2450-2463.
Tokarski, A. K., E. Marton, A. Swierczewska, A. Fheed, J. Zasadni, and J. Kukulak (2016), Neotectonic rotations in the Orava-Nowy Targ Intramontane Basin (Western Carpathians): An integrated palaeomagnetic and fractured clasts study, Tectonophysics, 685, 35-43.
Tontini, F. C., T. J. Crone, C. E. J. de Ronde, D. J. Fornari, J. C. Kinsey, E. Mittelstaedt, and M. Tivey (2016), Crustal magnetization and the subseafloor structure of the ASHES vent field, Axial Seamount, Juan de Fuca Ridge: Implications for the investigation of hydrothermal sites, Geophysical Research Letters, 43(12), 6205-6211.
Valet, J. P., L. Meynadier, Q. Simon, and N. Thouveny (2016), When and why sediments fail to record the geomagnetic field during polarity reversals, Earth and Planetary Science Letters, 453, 96-107.
Vissers, R. L. M., D. J. J. van Hinsbergen, D. G. van der Meer, and W. Spakman (2016), Cretaceous slab break-off in the Pyrenees: Iberian plate kinematics in paleomagnetic and mantle reference frames, Gondwana Research, 34, 49-59.
Volkova, V. S., O. B. Kuz'mina, and Z. N. Gnibidenko (2016), Position of the base of the Quaternary in West Siberia (based on paleobotanical and paleomagnetic evidence), Russian Geology and Geophysics, 57(9), 1312-1320.
Wang, H., Z. Y. Yang, Y. B. Tong, L. Gao, X. Q. Jing, and H. F. Zhang (2016), Palaeomagnetic results from Palaeogene

red beds of the Chuan-Dian Fragment, southeastern margin of the Tibetan Plateau: implications for the displacement on the Xianshuihe-Xiaojiang fault systems, International Geology Review, 58(11), 1363-1381.

Wang, B., G. W. Zhang, S. Z. Li, Z. Y. Yang, A. P. Roberts, Q. Zhao, and Z. Y. Wang (2016), Early Carboniferous paleomagnetic results from the northeastern margin of the Qinghai-Tibetan plateau and their implications, Gondwana Research, 36, 57-64.

Wang, W. T., P. Z. Zhang, J. Z. Pang, C. Garzione, H. P. Zhang, C. C. Liu, D. W. Zheng, W. J. Zheng, and J. X. Yu (2016), The Cenozoic growth of the Qilian Shan in the northeastern Tibetan Plateau: A sedimentary archive from the Jiuxi Basin, Journal of Geophysical Research-Solid Earth, 121(4), 2235-2257.

Petrophysics, Mineral Physics and Chemistry

Jarzyna, J. A., P. I. Krakowska, E. Puskarczyk, K. Wawrzyniak-Guz, J. Bielecki, K. Tkocz, J. Tarasiuk, S. Wronski, and M. Dohnalik (2016), X-ray computed microtomography-a useful tool for petrophysical properties determination, Computational Geosciences, 20(5), 1155-1167.

Johnson, J. R., et al. (2016), Constraints on iron sulfate and iron oxide mineralogy from ChemCam visible/near-infrared reflectance spectroscopy of Mt. Sharp basal units, Gale Crater, Mars, American Mineralogist, 101(7-8), 1501-1514.

Miller, W. G. R., T. J. B. Holland, and S. A. Gibson (2016), Garnet and Spinel Oxybarometers: New Internally Consistent Multi-equilibria Models with Applications to the Oxidation State of the Lithospheric Mantle, Journal of Petrology, 57(6), 1199-1222.

Senda, R., K. Shimizu, and K. Suzuki (2016), Ancient depleted mantle as a source of boninites in the Izu-Bonin-Mariana arc: Evidence from Os isotopes in Cr-spinel and magnetite, Chemical Geology, 439, 110-119.

Velasco, F., F. Tornos, and J. M. Hanchar (2016), Immiscible iron- and silica-rich melts and magnetite geochemistry at the El Laco volcano (northern Chile): Evidence for a magmatic origin for the magnetite deposits, Ore Geology Reviews, 79, 346-366.

Prospecting and Surveying

Anchuela, O. P., G. S. Miguel, B. Badenas, and M. Aurell (2016), Evaluation of pinnacle reef distribution at shallow subsurface using integrated geophysical methods: A case study from the upper Kimmeridgian (Spain), Marine and Petroleum Geology, 76, 329-343.

Asci, M., B. Dogan, T. Yas, and D. Caka (2016), Determination of the deep fault geometry along the southern branch of the North Anatolian Fault System by using resistivity and magnetic methods, Journal of Asian Earth Sciences, 125, 117-137.

Azeez, K. K. A. (2016), Magnetotelluric Constraints on the Occurrence of Lower Crustal Earthquakes in the Intra-plate Setting of Central Indian Tectonic Zone, Acta Geologica Sinica-English Edition, 90(3), 884-899.

Baptiste, J., G. Martelet, M. Faure, L. Beccaletto, P. A. Reninger, J. Perrin, and Y. Chen (2016), Mapping of a buried basement combining aeromagnetic, gravity and petrophysical data: The substratum of southwest Paris Basin, France, Tectonophysics, 683, 333-348.

Beka, T. I., M. Smirnov, Y. Birkelund, K. Senger, and S. G. Bergh (2016), Analysis and 3D inversion of magnetotelluric crooked profile data from central Svalbard for geothermal application, Tectonophysics, 686, 98-115.

Chen, X. B., and J. Y. Yan (2016), 2D magnetotelluric imaging of the Anqing-Guichi ore district, Yangtze metallogenic belt, eastern China: An insight into the crustal structure and tectonic units, Physics of the Earth and Planetary Interiors, 257, 1-11.

Gabas, A., A. Macau, B. Benjumea, P. Queralt, J. Ledo, S. Figueras, and A. Marcuello (2016), Joint Audio-Magnetotelluric and Passive Seismic Imaging of the Cerdanya Basin, Surveys in Geophysics, 37(5), 897-921.

Gessner, K., L. A. Gallardo, F. Wedin, and K. Sener (2016), Crustal structure of the northern Menderes Massif, western Turkey, imaged by joint gravity and magnetic inversion, International Journal of Earth Sciences, 105(7), 2133-2148.

Kwan, K., A. Prikhodko, J. M. Legault, G. C. Plastow, J. Kapetas, and M. Druecker (2016), VTEM airborne EM, aeromagnetic and gamma-ray spectrometric data over the Cerro Quema high sulphidation epithermal gold deposits, Panama, Exploration Geophysics, 47(3), 179-190.

Le, C. V. A., B. D. Harris, A. M. Pethick, E. M. T. Takougang, and B. Howe (2016), Semiautomatic and Automatic Cooperative Inversion of Seismic and Magnetotelluric Data, Surveys in Geophysics, 37(5), 845-896.

Legault, J. M., A. Latrous, S. K. Zhao, N. Bournas, G. C. Plastow, and G. G. Xue (2016), Helicopter AFMAG (ZTEM) EM and magnetic results over sedimentary exhalative (SEDEX) lead-zinc deposits at Howard's Pass in Selwyn Basin, Yukon, Exploration Geophysics, 47(3), 170-178.

Obiora, D. N., J. A. Yakubu, F. N. Okeke, J. U. Chukudebelu, and A. I. Oha (2016), Interpretation of Aeromagnetic Data of Idah Area in North Central Nigeria Using Combined Methods, Journal of the Geological Society of India, 88(1), 98-106.

Peron-Pinvidic, G., P. T. Osmundsen, and J. Ebbing (2016), Mismatch of geophysical datasets in distal rifted margin studies, Terra Nova, 28(5), 340-347.

Saibi, H., M. Azizi, and S. Mogren (2016), Structural Investigations of Afghanistan Deduced from Remote Sensing and Potential Field Data, Acta Geophysica, 64(4), 978-1003.

Selim, E., O. Abdel-Raouf, and M. Mesalam (2016), Implementation of magnetic, gravity and resistivity data in identifying groundwater occurrences in El Qaa Plain area, Southern Sinai, Egypt, Journal of Asian Earth Sciences, 128, 1-26.

Slezak, K., W. Jozwiak, K. Nowozynski, and H. Brasse (2016), 3-D Inversion of MT Data for Imaging Deformation Fronts in NW Poland, Pure and Applied Geophysics, 173(7), 2423-2434.

Xu, Y. X., S. Zhang, W. L. Griffin, Y. J. Yang, B. Yang, Y. H. Luo, L. P. Zhu, J. C. Afonso, and B. H. Lei (2016), How did the Dabie Orogen collapse? Insights from 3-D magnetotelluric imaging of profile data, Journal of Geophysical Research-Solid Earth, 121(7), 5169-5185.

Serpentinization

Bonnemains, D., J. Carlut, J. Escartin, C. Mevel, M. Andreani, and B. Debret (2016), Magnetic signatures of serpentinization at ophiolite complexes, Geochemistry Geophysics Geosystems, 17(8), 2969-2986.

Pens, M., M. Andreani, I. Daniel, J. P. Perrillat, and H. Cardon (2016), Contrasted effect of aluminum on the serpentinization rate of olivine and orthopyroxene under hydrothermal conditions, Chemical Geology, 441, 256-264.

Stratigraphy

Beluzhenko, E. V., and N. S. Pis'mennaya (2016), Upper Miocene-Eopleistocene terrestrial sediments of the northwestern Ciscaucasia region, Stratigraphy and Geological Correlation, 24(4), 407-426.

Bolikhovskaya, N. S., S. S. Faustov, and A. K. Markova (2016), Pleistocene climatic stratigraphy and environments of the Terek-Kuma Lowland (NW Caspian sea region) inferred from palynological, paleomagnetic and rodent records of the long Otkaznoye sediment sequence, Quaternary International, 409, 16-32.

Bujak, L., B. Woronko, H. Winter, B. Marcinkowski, T. Werner, R. Stachowicz-Rybka, M. Zarski, P. P. Wozniak, and O. Rosowiecka (2016), A new stratigraphic position of some Early Pleistocene deposits in central Poland, Geological Quarterly, 60(1), 238-251.

Fang, X. M., C. H. Song, M. D. Yan, J. B. Zan, C. L. Liu, J. G. Sha, W. L. Zhang, Y. Y. Zeng, S. Wu, and D. W. Zhang (2016), Mesozoic litho- and magneto-stratigraphic evidence from the central Tibetan Plateau for megamonsoon evolution and potential evaporites, Gondwana Research, 37, 110-129.

Lozovsky, V. R., Y. P. Balabanov, E. V. Karasev, I. V. Novikov, A. G. Ponomarenko, and O. P. Yaroshenko (2016), The terminal Permian in European Russia: Vyaznikovian Horizon, Nedubrovo Member, and Permian-Triassic boundary, Stratigraphy and Geological Correlation, 24(4), 364-380.

Musgrave, R. J., and M. Kars (2016), Recognizing magnetostratigraphy in overprinted and altered marine sediments: Challenges and solutions from IODP Site U1437, Geochemistry Geophysics Geosystems, 17(8), 3190-3206.

Peng, J., X. Q. Yang, X. K. Qiang, C. L. Liu, J. Li, Q. L. Lin, Y. Z. Weng, Q. X. Zhou, and J. Y. Ding (2016), Magnetostratigraphy characteristics of several cores around the Qiantang River mouth and its significance, Chinese Journal of Geophysics-Chinese Edition, 59(8), 2949-2964.

Song, C. H., Y. Y. Zeng, M. D. Yan, S. Wu, X. M. Fang, J. Bao, J. B. Zan, and X. F. Liu (2016), Magnetostratigraphy of the middle-upper Jurassic sedimentary sequences at Yanshiping, Qiangtang Basin, China, Geophysical Journal International, 206(3), 1847-1863.

Synthesis

Igarashi, K., Y. Yamamura, and T. Kuwabara (2016), Natural synthesis of bioactive greigite by solid-gas reactions, Geochimica Et Cosmochimica Acta, 191, 47-57.

cont'd. from pg. 1...

ropy of populations of settling magnetic particles.

The DRM vector is related to the applied field vector H by the DRM tensor k_D ($DRM = k_D H$), whose maximum and minimum elements (k_D max and k_D min) are respectively parallel to the horizontal and vertical components of H. The DRM components are then

$$DRM_x = k_D \max H_x$$
$$DRM_z = k_D \min H_z$$

Utilizing King's (1955) expression, the DRM inclination is related to the field inclination by

$$f = \frac{\tan I_{DRM}}{\tan I_F} = \frac{DRM_z / DRM_x}{H_z / H_x} = \frac{k_D \min}{k_D \max}$$

The DRM tensor is well approximated by the bulk remanent anisotropy (AARM), allowing Jackson et al. (1991) to develop a model relationship between the bulk AARM tensor (the minimum normalized principal value qz, in figure 2) and the flattening factor for magnetite particles of varying degrees of anisotropy (the individual particle anisotropy a factor).

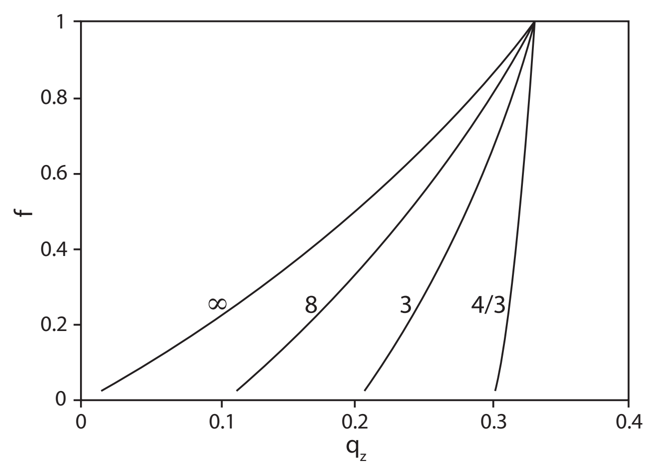

Fig. 2 Model relationship of Jackson et al. (1991) between DRM flattening factor *f* and ARM anisotropy for particle anisotropy values ranging from 4/3 to infinity. Note that the limiting case of *a*=1 corresponds to a vertical line at qz=1/3. One can have any amount of inclination shallowing, but there is no measurable ARM anisotropy resulting from the alignment of easy axes, because the particles are isotropic. For the other limiting case (*a*= infinity), the ARM tensor and the DRM tensor are identical.

The model is based on the idea that inclination shallowing depends only on the degree to which the particle remanent vectors are rotated toward the horizontal, whereas the ARM anisotropy of the population depends on both the degree of easy-axis alignment and the anisotropy of the individual particles. Tan and Kodama (2003) later adapted the model relationship (and correction equation) for the orientation distribution of platy hematite particles, for which the magnetic vector is constrained within the basal plane. The corrections of Jackson et al. (1991) and Tan and Kodama (2003) assumed that the shallowing only occurred within the X-Z plane (X is the remanent direction and Z is the vertical),

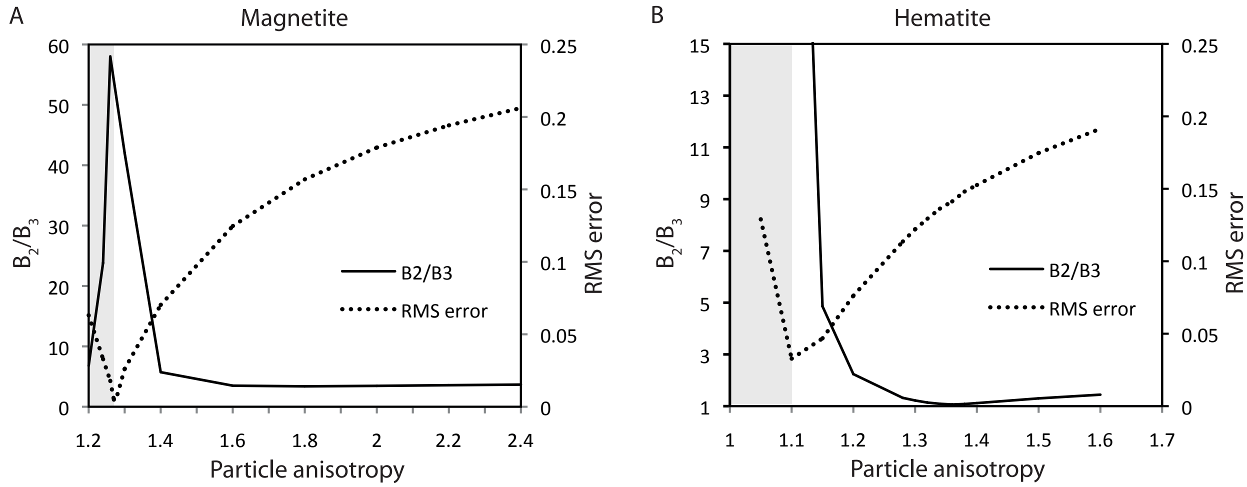

Fig. 3. A) RMS error (dotted curve) and Bingham B_2/B_3 axial ratio of the corrected directions (solid curve) for magnetite-bearing rocks (Deer Lake Group, Newfoundland, data from Bilardello and Kodama, 2010a), and B) RMS error (dotted curve) and Bingham B_2/B_3 axial ratio of the corrected VGPs for hematite bearing rocks (Shepody Formation, New Brunswick, Canada, data from Bilardello and Kodama, 2010b). The shaded boxes indicate the regions for which the inclination corrections do not work and the inclinations invert sign.

but Kim and Kodama (2004) developed a correction that also accounts for the slight orthogonal misalignment. All of these corrections are thus based on the measurement of the magnetic remanence and the magnetic anisotropy, with a preference for remanent anisotropy because it specifically targets the characteristic remanence carrying grains, though anisotropy of magnetic susceptibility may also be used.

The magnetic particle anisotropy factor *a*, is an essential quantity in all of these approaches and has been measured either from magnetic separates, assuming non-interaction of the grains (e.g. Vaughn et al., 2005) or estimated as described below.

Curve fitting technique

Tan and Kodama (2002) and Kodama (2009) estimated the particle anisotropy by iteratively varying the *a* factor in a curve fitting approach. The metric used is the RMS error of the analytical solution for *f* (Jackson et al. (1991) and Tan and Kodama (2003), for magnetite and hematite, respectively) for each sample/site and tan (I_R)/tan (I_M) calculated for each sample (or site), where I_R is the sample's (or site's) remanent inclination and I_M is the mean of the corrected inclinations. The value of *a* that yields the lowest RMS error should also be the value that yields the best fit of the corrected inclination data to the theoretical inclination shallowing curves for the measured anisotropy data (dotted curves in figure 3). Inclination correction data, however, seems to indicate that this approach is biased towards the smaller *a* factors: when a particle anisotropy used for the correction is too small with respect to the sample anisotropy, the correction ceases to work and yields inclinations that invert sign. The effect of these inverted inclinations is to dramatically increase the RMS. On the other hand, the RMS error always increases for increasing *a* values for which reasonable corrections are obtained, and this generates a minimum RMS for the smallest reasonable *a* value.

Elongation /Inclination technique

Tauxe and Kent (2004) instead developed a completely different approach presented in the very elegant Elongation/Inclination (*E/I*) technique. The distribution of virtual geomagnetic poles (VGPs) varies, as does the distribution of the magnetic directions, in accordance with the latitude at which the observations are made, following the Geocentric Axial Dipole hypothesis and paleosecular variation. This original distribution is altered during inclination shallowing, resulting in an E-W elongation of directions. The *E/I* technique performs bootstrap resampling of the directional data and iteratively varies the *f* factor to perform inclination corrections, generating corrected distributions of directions. The *f* factor that generates the corrected distribution that best fits the one predicted by the geomagnetic field model TK03 is used to determine the mean corrected inclination and bootstrapped confidence interval (high and low inclinations). The technique thus relies on the validity of the geomagnetic model and a relatively large number of samples (≥100) for the bootstrap distributions and confidence angles to be significant.

Distributions of directions and poles for anisotropy based corrections

Paleomagnetic samples that average secular variation within sampling sites should possess symmetrical distributions of site mean directions. Conversely, where secular variation has not been averaged within paleomagnetic sites, then symmetrical distributions of virtual geomagnetic poles (VGPs) are to be expected (Beck, 1999; Cox, 1964; Cox, 1970; Kono, 1997). Knowing the sediment accumulation rate of a rock formation allows one to estimate whether secular variation has been averaged within a site. One can then look at the symmetry of corrected paleomagnetic directions or VGPs generated using different a factors and determine the value that corresponds to the most symmetrical, and therefore most geologically reasonable, corrected distribution of directions or VGPs.

Bilardello and Kodama (2010a) performed anisotropy-based inclination corrections by progressively varying the a factor, and similarly to Tauxe and Kent (2005),

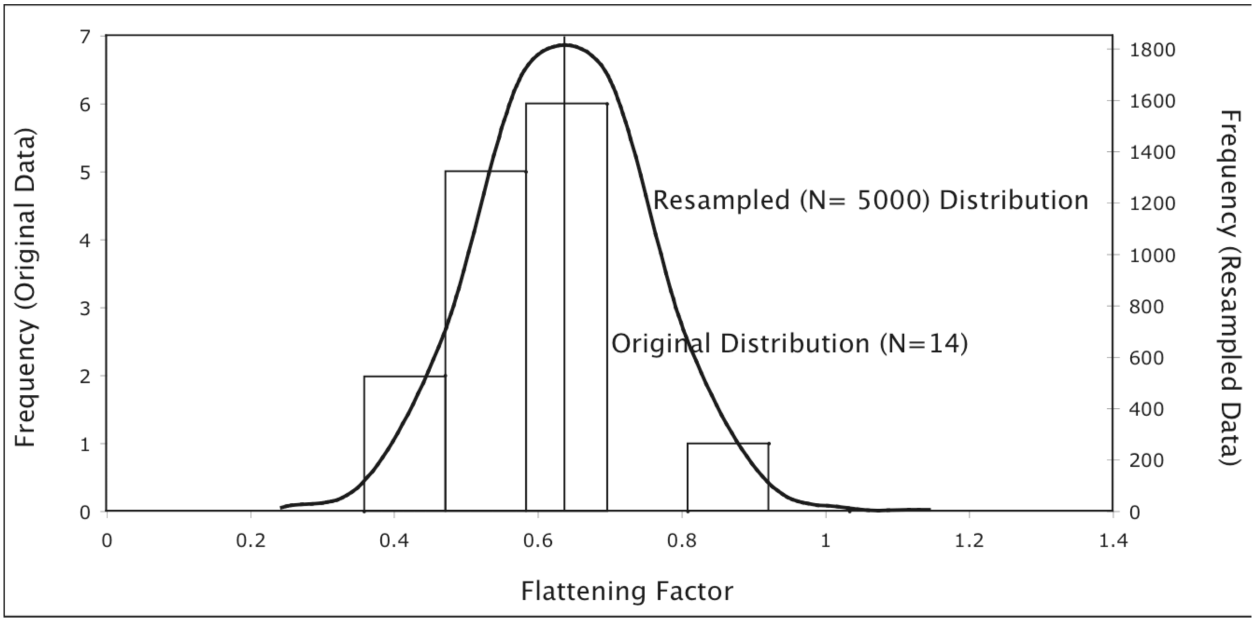

Fig. 4. Histogram showing the distribution of *f* factors determined from inclination correction studies of hematite-bearing rocks (from Bilardello, 2008 (unpublished). Boxes are the frequency distribution of the *f* factors (N=14) [data from Bilardello and Kodama (2010b), Tan et al. (2003) and Kent and Tauxe (2005)] plotted in bins that are one standard deviation- wide. The solid line was generated from random resampling of the data (5000x) using the measured mean and standard deviation following a normal distribution. This probability density function indicates a most likely *f* value of 0.64. This value falls within 1σ of the measured mean (0.58).

used the distribution of the corrected directions/VGPs to determine which value of *a* generates the most realistic distribution. For the rapidly deposited sediments they studied, they expected the most circular distribution of VGPs to yield the best correction. Bilardello and Kodama (2010a) estimated the circularity of both the distributions of directions and VGPs utilizing the Bingham distribution (Bingham, 1964) B2/B3 axial ratio: a minimum in this parameter is indicative of a more circular distribution. The *a* value was also measured directly from a magnetic extract and a value of 1.99 was obtained. On increasing the value of *a* the Bingham axial ratio of the directions yields a fairly flat curve for $a >$ 1.6, with a minimum at 1.8, in rough agreement with the magnetic extract, whereas the distribution of the VGPs yields the most symmetric distribution between 1.4 and 2.2. For these data the curve fitting approach instead determines a best *a* value of 1.28, which is also the first *a* value for which the correction works (Fig. 3a). For this *a* value the corrected inclinations are vertical. Interestingly it is the Bingham axial ratio of the corrected directions and not the VGPs that best agrees with the magnetic extract.

Bilardello and Kodama (2010b) performed a modified anisotropy-based inclination correction for fast deposited hematite-bearing sediment, for which a symmetric distribution of VGPs was expected. They also measured the particle anisotropy from magnetic extracts and obtained a mean value of 1.39. Performing the corrections and tracking the circularity of the distribution of poles by the Bingham axial ratio indicated a minimum at a=1.36. Instead the curve fitting approach gave a minimum at a=1.1, but for this value of *a* some of the corrected inclination already had inverted sign and the correction is thus deemed unreasonable (Fig. 3b).

For both these magnetite and hematite corrections the Bingham axial ratio returns the value of *a* that is in closest agreement to that obtained from magnetic separates, and realistic corrected inclination data.

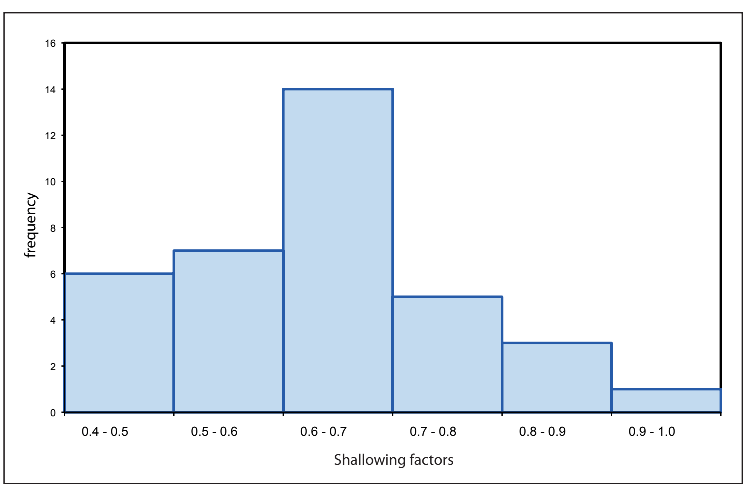

Fig. 5. Histogram of *f* factors derived from published inclination corrected data (N=36, bin size √N, mean= 0.65, mode= 0.49).

Distributions of estimated corrections

Bilardello and Kodama (2010a) compiled a list of flattening factors derived from hematite and magnetite inclination corrections. It is tempting to generate histograms and argue that if more data were available, or if the data were re-sampled, these had the potential of indicating normal distributions, and could in turn justify the use of mean *f* factors to perform simplified inclination corrections (figure 4). However, this approach should be avoided, because the flattening factor is in fact lithology-specific and no single value of *f* should be used to correct all existing rock-formations.

Bilardello and Kodama (2010c) discussed the lithology dependence of the *f* factor, and instead applied inclination corrections using the smallest *f* factors observed for hematite and magnetite, as part of an exercise to determine whether inclination shallowing could be responsible for misfit within particular Pangea models. An ongoing compilation of published *f* factors from inclination correction studies (N=36) shows that the distribution of data is skewed towards the smaller *f* factors, with a mode of 0.49 and a mean of 0.65 (figure 5). What this means is that blanket inclination-corrected data (performed using the mean *f* factor) will overall be under-corrected, while few data will also be over-corrected, introducing a new bias to published detasets.

Where do we go from here?

As new researchers weigh which inclination correction method to use in their own studies, it is important to consider which kinds of measurements different approaches require. The *E/I* technique of Tauxe and Kent (2004) is particularly attractive because it relies on the distribution of remanent directions in a study, and does not require additional anisotropy measurements or magnetic separation. However, it does require relatively large ($N \geq 100$) paleomagnetic datasets. By contrast, the anisotropy techniques can be used on smaller datasets, but require some additional measurements as well as a-priori information about the lithology, such as the depositional environment and settling rate, if the particle anisotropy has not been determined directly through magnetic separation techniques or other direct observations (e.g. Kodama, 2009). Learning to use inclination corrections is admittedly a steep learning curve, but recent work by various research groups has shown that our community is still in the process of refining our understanding of the mechanisms that control inclination shallowing. As our understanding improves, we're inclined (hopefully without error!) to believe that our correction tools will become more readily applicable to new users.

Acknowledgements

I thank Mike Jackson, Bruce Moskowitz and Josh Feinberg for their useful comments and suggestions.

References

Beck, M.E., 1999. On the shape of paleomagnetic data sets. J. Geophys. Res. 104, B11, 25,427-25,441.

Bilardello, D. and Kodama, K.P., 2010a. Rock magnetic evidence for inclination shallowing in the early Carboniferous Deer Lake Group red beds of western Newfoundland. Geophys. J. Int., 181, 275-289, doi: 10.1111/j.1365-246X.2010.04537.x.

Bilardello, D. and Kodama, K.P., 2010b. Paleomagnetism and magnetic anisotropy of Carbonifeous red beds from the Maritime Provinces of Canada: Evidence for shallow paleomagnetic inclinations and implications for North American apparent polar wander, Geophys. J. Int., 180, 3, 1013-1029, doi: 10.1111/j.1365-246X.2009.04457.x.

Bilardello, D. and Kodama, K.P., 2010c. A new inclination shallowing correction of the Mauch Chunk Formation of Pennsylvania, based on high field-AIR results: Implications for the Carboniferous North American APW path and Pangea reconstructions. Earth Planet. Sci. Lett., 299, 218-227, doi: 10.1016/j.epsl.2010.09.002.

Bingham, C., 1964. Distributions on the sphere and on the projective plane. Ph.D. Thesis, Yale University.

Cox, A., 1964. Angular dispersion due to random magnetization, Geophys. J. Roy. Astron. Soc., 8, 345-355.

Cox, A., 1970. Latitude dependence of the angular dispersion of the geomagnetic field. Geophys. J.R. Astron. Soc. 20, 253-269.

Garces, M., Pares, J.M., and Cabrera, L., 1996. Further evidence for inclination shallowing in red beds, Geophys. Res. Lett., 23, 2065-2068.

Griffiths, D. H., King, R. F., Rees, A. I. & Wright, A. E., 1960. Remanent magnetism of some recent varved sediments, Proc. R. Soc. A., 256, 359-383.

Jackson, M., Banerjee, S. K., Marvin, J.A., Lu, R. & Gruber, W., 1991. Detrital remanence inclination errors and anhysteretic remanence anisotropy: quantitative model and experimental results. Geophys. J. Int., 104, 95-103.

Kent, D. V., and Tauxe, L., 2005. Corrected late Triassic latitudes for continents adjacent to the North Atlantic. Science, 307, 240-244.

Kim, B. Y., Kodama, P.K., 2004. A compaction correction for the paleomagnetissm of the Nanaimo Group sedimentary rocks: Implications for the Baja British Columbia hypothesis. J. Geophys. Res., 109, B02102, doi:10.1029/2003JB002696.

King, R. F., 1955. The remanent magnetism of artificially deposited sediments, Mon. Notic. Roy. Astron. Soc. Geophys. Suppl. 7, 115-134.

Kodama, K. P., 2009. Simplification of the anisotropy-based inclination correction technique for magnetite- and hematite bearing rocks: A case study for the Carboniferous Gleshaw and Mauch Chunk Formations, North America. Geophys. J. Int., 176, 467-477, doi: 10.1111/j.1365-246X.2008.04013.x

Kono, M., 1997. Distributions of paleomagnetic directions and poles. Phys. Earth Planet. Int., 103, 313-327.

Tan, X. and Kodama, K.P., 2002. Magnetic anisotropy and paleomagnetic inclination shallowing in red beds: Evidence from the Mississippian Mauch Chunk Formation, Pennsylvania. J. Geophys. Res., 107 (B11), EPM 9, 17 pp.

Tan, X. and Kodama, K. P., 2003. An analytical solution for correcting paleomagnetic inclination error. Geophys. J. Int., 152, 228-236.

Tan, X., Kodama, K. P., Chen, H., Fang, D., Sun, D. and Li, Y., 2003. Paleomagnetism and magnetic anisotropy of Cretaceous red beds from the Tarim basin, northwest China: Evidence for a rock magnetic cause of anomalously shallow paleomagnetic inclinations from central Asia. J. Geophys. Res., 108, EPM 10, 20 pp.

Tauxe, L. and Kent, D.V., 1984. Properties of a detrital remanence carried by hematite from study of modern river deposits and laboratory redeposition experiments. Geophys. J. R. Astron. Soc., 77, 543-561.

Tauxe, L. and Kent, D.V., 2004. A simplified statistical model for the geomagnetic field and the detection of shallow bias in paleomagnetic inclinations: Was the ancient field dipolar? In: J.E.T. Channell, D.V. Kent, W. Lowrie and J. Meert, Editors, Timescales of the Internal Geomagnetic Field, Geophysical Monograph, 145, 101-116.

Vaughn, J., Kodama, K.P., and Smith, D.P., 2005. Correction of inclination shallowing and its tectonic implications: The Cretaceous Perforada Formation, Baja California. Earth Planet. Sci. Lett. 232, 71-82.

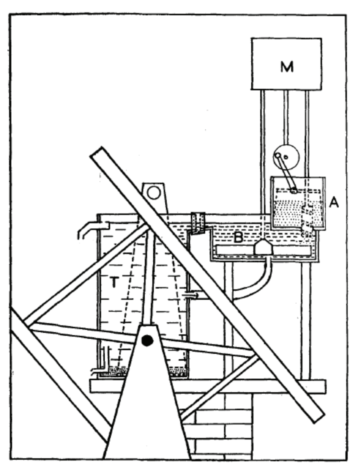

Sedimentation tank used by King (1955): A motor M, far enough not to affect the field generated in the Helmholtz coils drove a paddle in A, generating a water circulationn that allowed sediment in feeding tank B to be driven into the settling tank T. The three-feet Helmholtz coils were mounted on a pivot, allowing for a wide range of magnetic field directions.

University of Minnesota
291 Shepherd Laboratories
100 Union Street S. E.
Minneapolis, MN 55455-0128
phone: (612) 624-5274
fax: (612) 625-7502
e-mail: irm@umn.edu
www.irm.umn.edu

The IRM Quarterly

The *Institute for Rock Magnetism* is dedicated to providing state-of-the-art facilities and technical expertise free of charge to any interested researcher who applies and is accepted as a Visiting Fellow. Short proposals are accepted semi-annually in spring and fall for work to be done in a 10-day period during the following half year. Shorter, less formal visits are arranged on an individual basis through the Facilities Manager.

The *IRM* staff consists of **Subir Banerjee**, Professor/Founding Director; **Bruce Moskowitz**, Professor/Director; **Joshua Feinberg**, Assistant Professor/Associate Director; **Mike Jackson, Peat Sølheid** and **Dario Bilardello**, Staff Scientists.

Funding for the *IRM* is provided by the **National Science Foundation**, the **W. M. Keck Foundation**, and the **University of Minnesota**.

The *IRM Quarterly* is published four times a year by the staff of the *IRM*. If you or someone you know would like to be on our mailing list, if you have something you would like to contribute (*e.g.*, titles plus abstracts of papers in press), or if you have any suggestions to improve the newsletter, please notify the editor:

Dario Bilardello
Institute for Rock Magnetism
University of Minnesota
291 Shepherd Laboratories
100 Union Street S. E.
Minneapolis, MN 55455-0128
phone: (612) 624-5274
fax: (612) 625-7502
e-mail: dario@umn.edu
www.irm.umn.edu

University of Minnesota